Radar Detection in Coherent Multi-Sensor Multi-Frequency Systems

Salvatore Maresca
IEIIT Institute
National Research Council (CNR)
Pisa, Italy
salvatore.maresca@cnr.it

Antonio Malacarne
PNTLab Institute
Nat. Interuniv. Cons. for Telecom. (CNIT)
Pisa, Italy
antonio.malacarne@cnit.it

Malik Muhammad Haris Amir
TeCIP Institute
Sant'Anna School of Advanced Studies (SSSA)
Pisa, Italy
malikmuhammadharis.amir@santannapisa.it

Fawad Ahmad
TeCIP Institute
SSSA
Pisa, Italy
fawad.ahmad@santannapisa.it

Gaurav Pandey
TeCIP Institute
SSSA
Pisa, Italy
gaurav.pandey@santannapisa.it

Antonella Bogoni
PNTLab Institute
CNIT
Pisa, Italy
antonella.bogoni@cnit.it

Mirco Scaffardi
PNTLab Institute
CNIT
Pisa, Italy
mirco.scaffardi@cnit.it

***Abstract*—In this paper, two types of multi-sensor multi-frequency radar systems are simulated in a close-to-reality maritime surveillance scenario for detecting extended naval targets.**

The first type of system is a multiple-input multiple-output (MIMO) radar with separated antennas. Such system, which employs multiple spatially distributed transmit (TX) and (RX) nodes, maximizes the information content extracted from each signal by means of a centralized data fusion procedure. The second type of system is a multistatic radar, which instead implements a decentralized information fusion procedure.

Both radar network architectures are simulated in the MATLAB® programming environment and their detection capabilities, evaluated in terms of probability of detection and probability of false alarm, analyzed at the varying of different operating parameters.

***Index Terms*—Multiple-Input Multiple-Output Radar, Multistatic Radar, Multi-Frequency System, Target Detection, Radar Cross Section.**

I. Introduction

Next generation radar surveillance systems will be based on multiple radar apparatuses distributed in space and exploiting information diversity. Such systems, commonly called multistatic radars [1], rely on the concept of information fusion for improving not only target detection capability in the presence of radar cross section (RCS) fluctuations, but also the tracking and imaging capabilities of the system.

In particular, a multistatic radar system can be described as a network of distributed (i.e., widely separated) transmit (TX) and receive (RX) antennas. The distributed nature of the system allows to exploit multiple points of view for observing the same target of interest. However, the limitation of such systems is that, even though multiple radar heads (RHs) are used, they rarely cooperate with each other. In fact, the received signals are usually locally pre-processed at each RH, and the outcomes are sent to the central unit (CU) for implementing fusion of information extracted from the data processed in a decentralized manner.

Similar to multistatic systems, multiple-input multiple-output (MIMO) radars employ multiple spatially distributed TX and RX nodes. However, they exhibit an higher degree of system cooperativeness. In fact, in these systems, the raw received signals are directly sent to the CU. This, at least in theory, allows to maximize the information content extracted from each signal by means of a centralized data fusion procedure [2], [3].

This paper investigates the performance of a coherent multi-frequency MIMO radar network in detecting extended naval targets in a close-to-reality scenario (i.e., a port). Then, the MIMO radar system, which relies on photonics-based optical generation, distribution and detection of the radar signals [4], [5], is compared with a multistatic radar employing the same RHs, but using a decentralized processing architecture.

The results presented in this paper are carried out based on a simulation tool in MATLAB® environment, specifically developed to investigate the performance of coherent multi-frequency MIMO radar systems.

The paper is organized as follows. In Section II, multi-sensor radar detection is presented. In Section III, the simulation scenario is described, whereas simulation results are shown and discussed in Section IV. Finally, comments are provided in Section V.

The project leading to this pubblication has received funding from Frontex under the Frontex Research Grants Programme. Call for Proposals 2022/CFP/RIU/01 - Grant Agreement No. 2023/350. This pubblication reflects only the authors' view. Neither the European Union nor Frontex are responsible for any use that may be made of the information it contains.

This work has also been partially funded by the EU under the Italian National Recovery and Resilience Plan (PNRR) of NextGenerationEU partnership on "Telecommunications of the Future" (PE00000001 - program "RESTART").

II. Multi-Sensor Radar Detection

Let us consider a general multi-sensor radar system employing M transmit and N receive antenna elements, not necessarily co-located. The front-ends are denoted with TX_m and RX_n, being $m = 1, \ldots, M$ and $n = 1, \ldots, N$, with $M \neq N$. For generality, TX_m can operate at L different radio frequencies (RFs). The received signal model for a general multi-sensor radar system can be written in the following matrix product form:

$$\mathbf{r}(t) = \sqrt{\frac{E}{M}} \text{diag}\left[\mathbf{b}(x_0, y_0)\right] \mathbf{s}(t - \tau) + \mathbf{n}(t), \tag{1}$$

where $\mathbf{s}(t)$ is the transmitted signal, such that $\|\mathbf{s}(t)\|^2 = 1$; τ is the target delay observed at the receiver; $\mathbf{H}$ is the channel matrix, such that $[\mathbf{H}]_{lk} = \alpha_{lk}$; diag$(\mathbf{v})$ is a diagonal matrix with $\mathbf{v}$ on its diagonal; $\mathbf{a}(x_0, y_0) = \left[1, e^{j\phi_2}, \ldots, e^{j\phi_N}\right]^T$ is the $N \times 1$ receiver steering vector, which is a function of the target location (x_0, y_0); $\mathbf{b}(x_0, y_0) = \left[1, e^{j\psi_2}, \ldots, e^{j\psi_M}\right]^T$ is the $M \times 1$ transmitter steering vector, and E is the total average received energy.

Finally, $\mathbf{n}(t) = [n_1(t), \ldots, n_N(t)]^T$ is a $N \times 1$ vector representing the additive noise. We assume that is a white, zero-mean, complex normal random process with correlation matrix $\sigma_n^2 \mathbf{I}_N$, where $\mathbf{I}_N$ is the $N \times N$ identity matrix.

Multi-sensor radar systems essentially differ in two aspects: the correlation between the elements of the channel matrix and the design of the transmitted signals. In [6], the Authors consider four canonical systems, representing four extreme cases. These four systems are the conventional phased-array radar, the MIMO radar, and the multiple-input single-output (MISO) and the single-input multiple-output (SIMO) radars.

In this paper, multistatic radars will be compared with coherent MIMO radars. The optimal detector, in the Neyman–Pearson sense, is the likelihood ratio test (LRT), which is described by [7]:

$$T = \log\left[\frac{f(\mathbf{r}(t)|H_0)}{f(\mathbf{r}(t)|H_0)}\right] \underset{<H_0}{\gtrless^{H_1}} \delta, \tag{2}$$

where $f(\mathbf{r}(t)|H_0)$ and $f(\mathbf{r}(t)|H_0)$ are the probability density functions (PDFs) of the observation vector $\mathbf{r}(t)$ given the *target absent* and *target present* hypotheses, respectively, and δ is a threshold, set by the desired probability of false alarm P_{FA}. Since we are interested in comparing the detection capabilities of MIMO and multistatic radar systems, we assume that the noise level is known in advance.

A. Detection for MIMO Radars

For MIMO radars, the optimal detector is given by [6]:

$$T = \|\mathbf{x}\|^2 \underset{<H_0}{\gtrless^{H_1}} \delta, \tag{3}$$

where

$$\|\mathbf{x}\|^2 \sim \begin{cases} \frac{\sigma_n^2}{2}\chi^2_{2MN}, & H_0 \\ \left(\frac{E}{2M} + \frac{\sigma_n^2}{2}\right)\chi^2_{2MN}, & H_1 \end{cases} \tag{4}$$

and where χ^2_{2MN} denotes a chi-square random variable with $2MN$ degrees of freedom. The probability of false alarm P_{FA} can be expressed as:

$$P_{FA} = \Pr\{T > \delta | H_0\} = \Pr\left\{\chi^2_{2MN} > \frac{2\delta}{\sigma_n^2}\right\}. \tag{5}$$

It follows that δ is set using the following formula:

$$\delta = \frac{\sigma_n^2}{2} F^{-1}_{\chi^2_{2MN}}\left(1 - P_{FA}\right), \tag{6}$$

where $F^{-1}_{\chi^2_{2MN}}$ denotes the inverse cumulative distribution function of a chi-square random variable with $2MN$ degrees of freedom.

Finally, the probability of detection P_D is given by:

$$\begin{aligned} P_D &= \Pr\{T > \delta | H_1\} = \\ &= 1 - F_{\chi^2_{2MN}}\left[\frac{\sigma_n^2}{E/M + \sigma_n^2} F^{-1}_{\chi^2_{2MN}}\left(1 - P_{FA}\right)\right]. \end{aligned} \tag{7}$$

As highlighted in [6], it is interesting to note that both the test statistic, see eq. (3), and the threshold, see eq. (6), are independent of the transmitted energy. Therefore, the optimal detector, even in the case of unknown signal energy, is given by eq. (3) and eq. (6). This establishes the fact that eq. 3 describes a uniformly most powerful (UMP) detector for which only the noise level needs to be known [8]. Closed-form formulas for eqs. (3), (6), and (7) are reported in [9].

B. Detection for Multistatic Radars

Unlike MIMO radars, the detection capability of multistatic radars is evaluated for each transmitter-receiver pair and then the final probability of detection is found by a decision over all local probabilities [10]. In fact, the multistatic radar processes received signals locally at each receiver and then a fusion center gets the thresholded signals for higher order decisions such as detection.

The local probability of false alarm and the probability of detection for every pair can be computed using the Swerling equations as:

$$P_{FA}^{(p)} = \exp\left(-\frac{\varsigma^2}{2}\right), \tag{8}$$

$$P_D^{(p)} = \exp\left[-\frac{\varsigma^2}{2\left(1 + SNR_p\right)}\right], \tag{9}$$

with SNR_p being the target SNR in the p-th pair of transmitters and receivers. The probability vector

$$P_D = \left[P_D^{(1)}, \ldots, P_D^{(MN)}\right]^T \tag{10}$$

is defined to characterize the local detection information for each pair. The m/n logic, where $m = K$ and $n = MN$, with $n \leq n$, can be used to calculate the total probability of detection [11]:

$$\begin{aligned} P_D^{tot} = \\ \sum_{l=K}^{MN}\left[\sum_{p=0}^{l-K}(-1)^p\binom{l}{p}\right]\left[\sum_{c\in C_{L,MN,0}}\left(\prod_c P_D^{(c)}\right)\right], \end{aligned} \tag{11}$$

where $C_{L,MN,0}$ denotes all the possible c permutations of the set $[1, 2, \ldots, MN]$.

III. Simulation Scenario

The simulation scenario is modelled considering three radar heads (RHs), all acting as transceivers operating both in monostatic and bistatic configurations. The RHs are deployed in the port of Livorno, Italy, for detecting the traffic entering the port from south, mimicking the coherent MIMO radar network demonstrator presented in [12], [13].

The geodetic coordinates of the RHs are as follows:

- **RH1**: $[10°17'29.6''\text{E}, 43°33'30.1''\text{N}]$,
- **RH2**: $[10°17'50.1''\text{E}, 43°33'11.2''\text{N}]$,
- **RH3**: $[10°17'45.3''\text{E}, 43°32'57.3''\text{N}]$,

Fig. 1 shows the Livorno port area map. The triangles identify the locations of the RHs, and the piecewise line the target vessel trajectory. The target RCS is modelled according to the procedure described in [14], which is based on the MATLAB® tool POfacets [15], [16].

With the RH1 location serving as the local East-North-Up (ENU) reference system's centre, the problem of target detection and localization is transferred from the World Geodetic System 1984 (WGS-84) to the ENU coordinate system for ease of description. System parameters are summarized in Table I.

Parameter	Value
RF carriers	8, 9, 10 GHz
Modulation	Linear Freq. Mod. (LFM) Pulse
Bandwidth	600 MHz
Pulse rep. interval (PRI)	20μs
Pulse duration	200 ns
Transmitted power	20 W
RH antenna gain	20 dBi
Target length	10, 25, 50 m
Fiber length (from CU to RHs)	5 km
Target RCS	Based on target position along path

TABLE I
MIMO/MULTISTATIC RADAR SYSTEM PARAMETERS

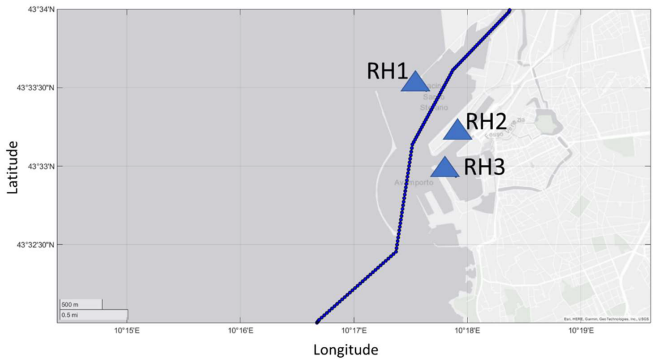

Fig. 1. Map of the Livorno port area. The radar system is composed by three radar heads (RHi). The line corresponds to the trajectory of a vessel entering the port.

IV. Simulation Results

The comparison between MIMO and multistatic detectors is conducted evaluating the probability of detection for the different radar configurations at each vessel position. In particular, three study cases are considered.

- *Study Case A*: comparison of single-band MIMO radar with single-band multistatic radars;
- *Study Case B*: comparison of single-band MIMO with three-band MIMO radar;
- *Study Case C*: comparison of three-band MIMO with three-band multistatic radar.

A. Single-band MIMO radar vs. single-band multistatic radar

In this section, the single-band MIMO radar system is compared with the single-band multistatic system. The comparison is done for all the radar carrier frequencies, i.e., 8, 9 and 10 GHz, and results are shown in Fig. 2.

The probability of detection, as expected, is larger for vessels of larger dimension. The coherent MIMO performs better than the multistatic radar at all the considered RF carriers and for all the vessel sizes.

Both the MIMO and the multistatic radar have lower probability of detection for higher carrier frequency, but the performance worsening in the coherent MIMO radar is smaller and present only at the edges of the probability of detection curve as a function of the target position, and does not affect the maximum of the curve.

B. Single-band vs. three-band MIMO radar

The comparison between the single-band and the three-band coherent MIMO radar is done for three vessels of 10, 25 and 50 m length. The considered radio frequencies (RFs) are, again, 8, 9 and 10 GHz. Results are shown in Fig. 3.

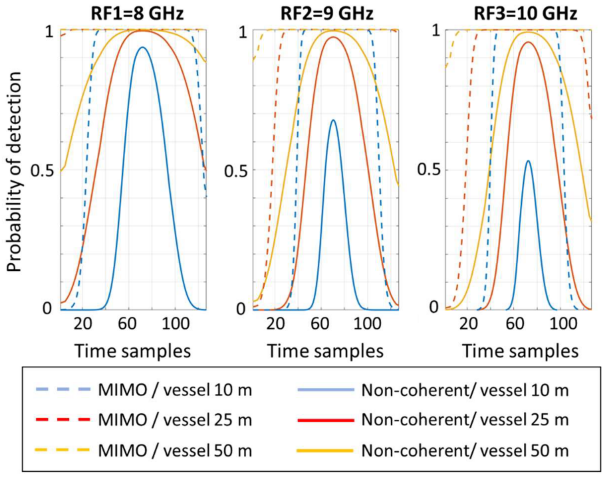

Fig. 2. Probability of detection for the single-band coherent MIMO radar and the multistatic non-coherent radar for RF carrier at 8, 9, and 10 GHz and for target vessels of 10, 25 and 50 m length. Curves are represented vs. time, i.e., different vessel position with respect to the scenario of Fig. 1.

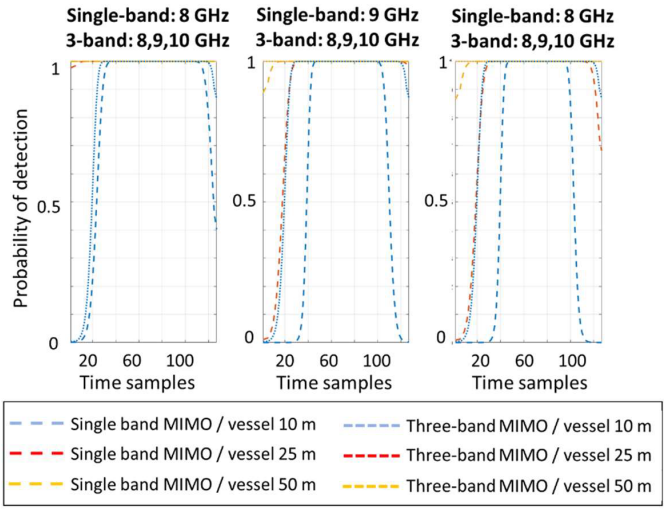

Fig. 3. Probability of detection for the single-band and the three-band coherent MIMO radar. Vessels of length 10, 25 and 50 m are considered. Carrier frequencies are 8, 9, and 10 GHz. Curves are represented vs. time, i.e., different vessel position with respect to the scenario of Fig. 1.

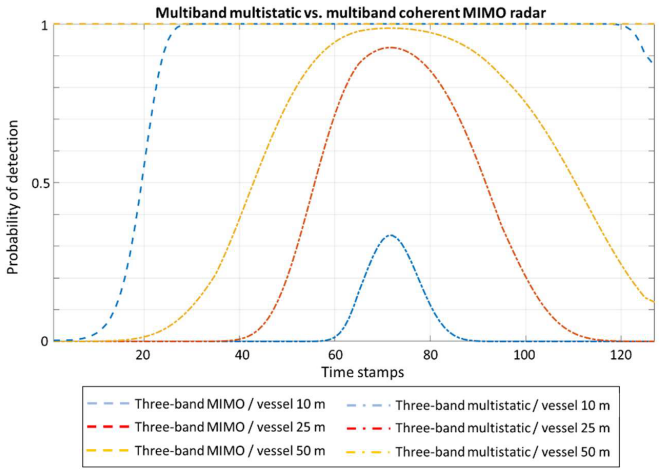

Fig. 4. Probability of detection for the three-band coherent MIMO and the three-band multistatic radar. Vessels of length 10, 25 and 50 m are considered. Carrier frequencies are 8, 9, and 10 GHz. Curves are represented vs. time, i.e. different vessel position with respect to the scenario of Fig. 1.

For both the single-band and three-band MIMO radars the probability of detection is at maximum for a large time interval (i.e., vessel positions). For the three-band MIMO radar the time interval at which the probability of detection is maximum is larger than for the single-band MIMO radar for all the considered vessels dimensions.

C. Three-band MIMO radar vs. three-band multistatic radar

In this section, the three-band coherent MIMO radar is compared with the three-band multistatic radar, considering the same vessel lengths and RF carriers. As shown in Fig. 4, the three-band coherent MIMO radar has higher probability of detection than the three-band multistatic radar for all the considered vessels positions and for all the vessels sizes.

Moreover, the three-band coherent MIMO has a probability of detection that is maximum and equal to 1 for almost the whole observation interval for vessels of 25 and 50 m, while for a large interval for smaller vessels of 10 m. The total radar system probability of detection shown in Fig. 4 results from the contribution of each couple of bistatic radar channels and for each carrier frequency.

The probability of detection of the individual contributions of all the frequencies and channels (RHs) is shown in Fig. 5. For some target positions and some bistatic couple and frequencies, the resulting P_D is very low. Nevertheless, the coherently combined ambiguity functions results into a very high probability of detection, as shown in Fig. 4.

V. Conclusion

In this paper, two types of multi-sensor multi-frequency radar systems have been simulated in a close-to-reality maritime surveillance scenario for detecting extended naval targets. The first type of system is a multiple-input multiple-output (MIMO) radar with separated antennas and employs a centralized radar network architecture. The second type of system is a multistatic radar, which instead implements a decentralized information fusion procedure. Both radar network architectures have been simulated in the MATLAB® programming environment and their performance, evaluated in terms of probability of detection and probability of false alarm, analyzed at the varying of different operating parameters (i.e., target location, target length, carrier frequencies).

In terms of bandwidth, the single-band MIMO performed better than the multistatic radar at all the considered RF carriers (i.e., 8, 9 and 10 GHz) and for all the considered ship sizes (10, 25 and 50 m). Both the MIMO and the multistatic radars achieved lower probability of detection for higher carrier frequency, but the performance worsening in the coherent MIMO radar was smaller and present only at the edges of the probability of detection curve as a function of the target position, not affecting the maximum of the curve.

In terms of multi-frequency operation comparison, for the three-band MIMO radar, the time interval at which the probability of detection is maximum was larger than for the single-band MIMO radar for all the considered target vessel dimensions. Among a coherent three-band MIMO radar and a three-band multistatic radar, the three-band MIMO radar has higher probability of detection for all the considered target vessels positions and sizes. Moreover, the three-band MIMO had a unitary probability of detection for almost the whole observation interval for vessels of 25 and 50 m, while for a large interval for smaller vessels of 10 m.

Additional results and further comments will be provided in the final version of the paper.

References

[1] V. S. Chernyak, Fundamentals of Multisite Radar System, 1998.
[2] E. Fishler, *et al.*, "MIMO radar: An idea whose time has come," *IEEE Radar Conf.*, pp. 71–78, 2004.

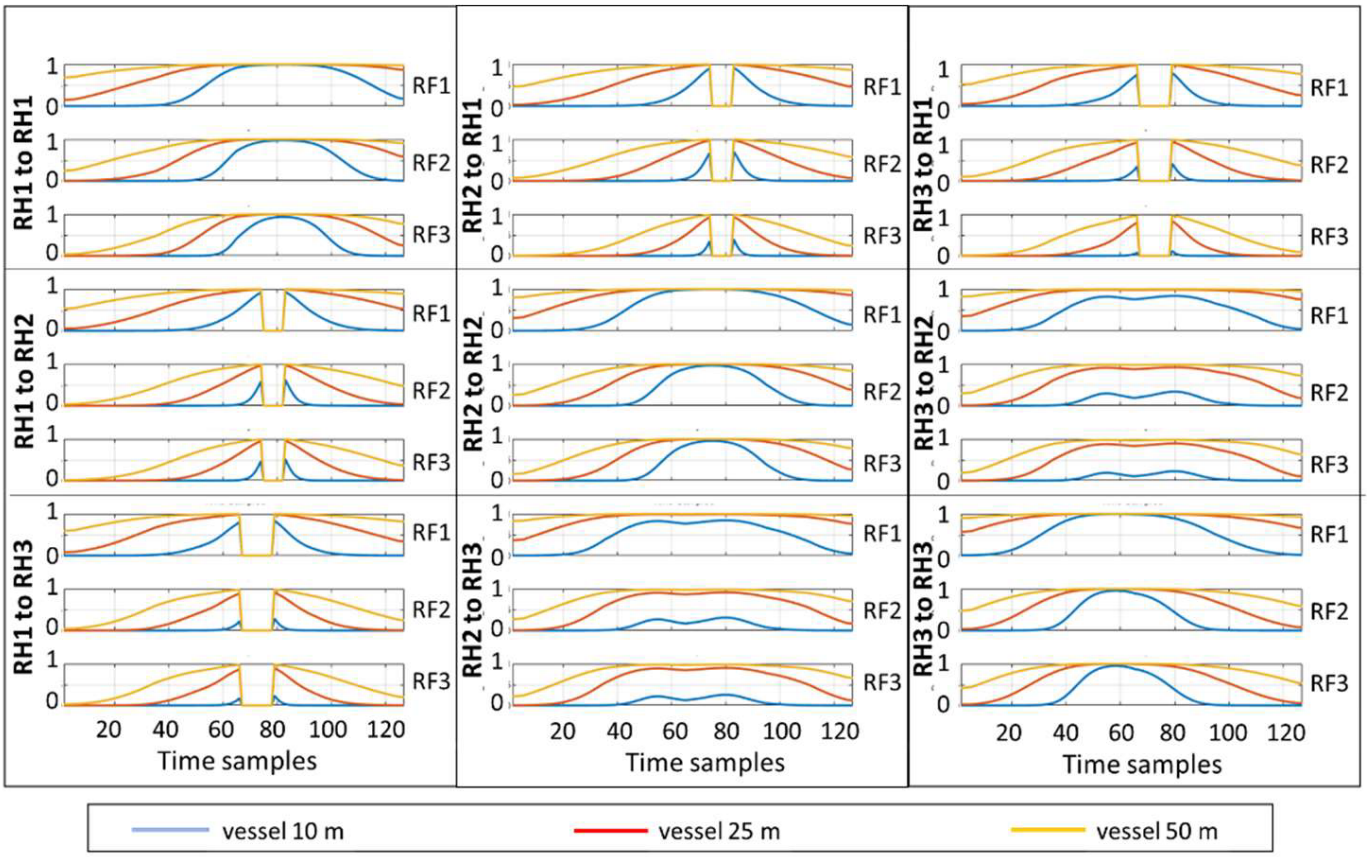

Fig. 5. Probability of detection for the individual frequencies and each couple of bistatic channels (RH couple) at different vessels length (10, 25 and 50 m).

[3] A. M. Haimovich, *et al.*, "MIMO Radar with Widely Separated Antennas," *IEEE Sig. Proc. Mag.*, vol. 25, no. 1, pp. 116-129, 2008.

[4] G. Serafino, *et al.*, "Toward a New Generation of Radar Systems Based on Microwave Photonic Technologies," in Journal of Lightwave Technology, vol. 37, no. 2, pp. 643-650, 15 Jan.15, 2019.

[5] G. Serafino, *et al.*, "Microwave Photonics for Remote Sensing: From Basic Concepts to High-Level Functionalities", *IEEE J. of Light. Tech.*, vol. 38, no. 19, pp. 5339-5355, 2020.

[6] E. Fishler, A. Haimovich, R. S. Blum, L. J. Cimini, D. Chizhik, and R. A. Valenzuela, "Spatial Diversity in Radars—Models and Detection Performance," in IEEE Transactions on Signal Processing, vol. 54, no. 3, pp. 823-838, March 2006.

[7] H. L. V. Trees, Detection, Estimation, and Modulation Theory. New York: Wiley, 1968, vol. I.

[8] E. L. Lehmann, Testing Statistical Hypotheses, 2nd ed. New York: Wiley, 1986.

[9] M. Abramowitzm and I. A. Stegun, Handbook of Mathematical Functions with Formulas, Graphs, and Mathematical Tables, 9th ed. New York: Dover, 1972.

[10] A. A. Gorji, R. Tharmarasa, and T. Kirubarajan, "Widely Separated MIMO versus Multistatic Radars for Target Localization and Tracking," in IEEE Transactions on Aerospace and Electronic Systems, vol. 49, no. 4, pp. 2179-2194, Oct. 2013.

[11] F. Gini, F. Lombardini, and P. K. Varshney, "On distributed signal detection with multiple local free parameters," in IEEE Transactions on Aerospace and Electronic Systems, vol. 35, no. 4, pp. 1457-1466, Oct. 1999.

[12] G. Serafino, *et al.*, "A Photonics-Assisted Multi-Band MIMO Radar Network for the Port of the Future," in IEEE Journal of Selected Topics in Quantum Electronics, vol. 27, no. 6, pp. 1-13, Nov.-Dec. 2021, Art no. 6000413.

[13] S. Maresca, *et al.*, "Field Trial of a Coherent, Widely Distributed, Dual-Band Photonics-Based MIMO Radar With ISAR Imaging Capabilities," in Journal of Lightwave Technology, vol. 40, no. 20, pp. 6626-6635, 15 Oct.15, 2022.

[14] M. M. H. Amir, *et al.*, "Modelling of Extended Targets with Dual-Band MIMO Radar Networks," 2021 18th European Radar Conference (EuRAD), London, United Kingdom, 2022, pp. 345-348.

[15] F. Chatzigeorgiadis, *Development of Code for a Physical Optics Radar Cross Section Prediction and Analysis Application*, Sept. 2004.

[16] D. Jenn, POfacets4.3 MATLAB Central File Exchange, [online] Available: https://www.mathworks.com/matlabcentral/fileexchange/50602-pofacets43.